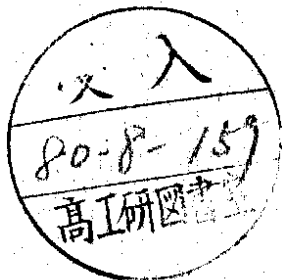


DEUTSCHES ELEKTRONEN-SYNCHROTRON **DESY**

DESY 80/64
July 1980



TECHNOLOGY OF DRIFT CHAMBERS

by

D. Schmidt

*Gesamthochschule Wuppertal
and*

Deutsches Elektronen-Synchrotron DESY, Hamburg

NOTKESTRASSE 85 · 2 HAMBURG 52

DESY behält sich alle Rechte für den Fall der Schutzrechtserteilung und für die wirtschaftliche Verwertung der in diesem Bericht enthaltenen Informationen vor.

DESY reserves all rights for commercial use of information included in this report, especially in case of apply for or grant of patents.

**To be sure that your preprints are promptly included in the
HIGH ENERGY PHYSICS INDEX ,
send them to the following address (if possible by air mail) :**

**DESY
Bibliothek
Notkestrasse 85
2 Hamburg 52
Germany**

Technology of Drift Chambers[†]

by

D. Schmidt

Gesamthochschule Wuppertal
and

Deutsches Elektronen-Synchrotron DESY, Hamburg

Abstract

The technical realization of wire chambers, starting from physical principles, is discussed. Problems specific to different chamber types are emphasized.

In the last 10 to 15 years starting from the pioneering work of Charpack and coworkers the use of drift chambers has steadily increased in various experiments. Large complex arrangements are common in high energy set ups nowadays. Various different types were developed in the past and today, it seems to me that even new series of gaseous detectors are in the testing stage, for example parallel plate structures, multigaps and so on.

In this paper I would like to discuss only those types which have already been used in large quantities in experimental arrangements and have shown their reliability.

The conventional drift chambers to which I will restrict myself have now reached a rather high stage of development. I would like to summarise various techniques being used in chamber construction. Two examples of cylindrical chambers will be shown, one working at normal and the other at high pressure. Besides these a high resolution planar chamber will be discussed. At the end of this paper I would like to present a poor man's chamber which is inexpensive but still maintains a reasonable spacial resolution. This type is suitable for large area experiments detecting muons.

But before going into details of the chamber construction I would like to discuss the theoretical accuracy of the position measurements because this determines how carefully the chambers must be built.

Limitation on the position measurements

For known velocity v of the drifting electrons the position x is given by

$$x = \int_{t=t_0}^{t=t_1} v dt = f\left(\frac{E}{M}\right) + f\left(\frac{E}{p}\right) \quad T=\text{const}$$

where t_0 is the time of the production of primary ions by a charge particle, t_1 is the time at which the electrons reach the sense wire, E , M , p and I are the electric field, number of molecules per cm^3 , pressure and temperature, respectively. For gas composition such that the velocity is independent of E the relation simply reduces to $x = (t_1 - t_0) v$.

[†] Invited talk, given at the 1980 Wire Chamber Conference, Vienna, Austria, 27-29 February 1980

What are the limiting factors in measuring the position of the primary particles? The answer to that question can be found in many articles, for example in a beautiful publication by Sauti¹.

The spacial resolution as a function of the drift path x depends mainly on four components:

$$\sigma^2(x) = \sigma_{\text{track}}^2 + \sigma_{\text{ion}}^2(x) + \sigma_{\text{diff}}^2(x) + \sigma_{\text{electron}}^2$$

σ_{track} depends on the physical track width which is mainly determined by the range of the produced δ electrons and the associated γ -rays. The number of electrons with kinetic energy equal to or larger than E_0 is given in first order approximation by

$$N(E > E_0) = \frac{K \cdot Z}{g^2 \cdot A} \rho d \left(\frac{1}{E_0} - \frac{1}{E_M} \right)$$

where Z , A , c and d are the atomic number, weight, density and thickness of the gas and E_M is the maximum possible energy transfer in that interaction. In going to higher density (that means increasing the pressure p) the range of the δ electrons decreases but as can be seen from the formula their number increases. The resulting effect can be seen in fig. 1. The curves a) and b) at different pressures but at the same gas volume thickness clearly show the increasing influence of the δ electrons with increasing pressure. Curve c) shows the direct dependence of δ -ray number on chamber thickness. σ_{track} is of course independent of the drift path x .

The second term σ_{ion} is due to fluctuations of primary ionization density. This influences the space resolution mainly for tracks close to the sense wire. At $x = 0$ one gets $\sigma_{\text{ion}}^2(x=0) = 1/(2 N^2)$ where N is the number of primary ionization clusters per cm. When the gas pressure increases N gets larger and σ_{ion} decreases.

The third factor σ_{diff} stems from the diffusion of an electron drifting along the path x

$$\Delta x = \sqrt{2 D \frac{x}{\mu} \cdot \frac{x}{E}} = f \left(\frac{p}{E} \right) \sqrt{\frac{x}{p}}$$

D , μ are the diffusion constant and the electron mobility of the chamber gas. The effect of this diffusion will be reduced since the commonly used drift chamber electronics are almost sensitive to the first electron reaching the sense wire, making

$$\sigma_{\text{dif}} \approx \frac{0.9}{\sqrt{\ln n}} \cdot \Delta x \quad \text{where } n \text{ is the number of primary electrons in a cluster.}$$

These relations show that the diffusion term contributes increasingly with the drift path x . At a constant v (that means at a constant value of p/E) the value of σ_{diff} decreases with increasing pressure p .

The last term σ_{el} takes into account the effects of the time measuring electronics.

Besides these statistical errors systematic deviations may contribute, for example uncertainty in the exact value of the drift velocity. But since these effects will not influence the chamber construction I will not discuss them here.

Fig. 2 presents the experimentally determined track measurement error as a function of drift distance as measured by Schulz². The increase in the error at small drift distance due to the fluctuation of the primary statistics is clearly visible. At large x the diffusion term starts to dominate as expected. Using higher pressures σ_{ion} and σ_{diff} decrease but σ_{track} could increase. The net effect is shown in fig. 3. These results were obtained by a group at Heidelberg³ who did pioneering work in drift-chamber development. With increasing pressure the positioning accuracy is improved. Accuracies up to 30 μm were obtained.

What conclusions affecting chamber construction can be drawn from these considerations? Specific answers will be given in discussing the various chamber types, but as a general rule in building the most accurate chambers with resolutions of 20 to 30 μm the drift path should be only a few centimeters (diffusion), the gap should be rather thin (δ electrons) and the pressure should be high.

Before going into details in describing the performance of different chamber types I would like to make some general remarks about chamber construction.

General principles in chamber construction

The sense wire is one of the main parts in a drift chamber. The first question is what kind of wire should be used.

The diameter should be small in order to create the high electric field needed for electron amplification. The smaller the diameter the smaller the necessary applied voltage. But there are physical limits. 20 μm is the smallest practical

diameter. For long wires the ohmic resistance becomes non-negligible and attenuation of the output pulses must be considered. In fact this feature is sometimes used in determining the coordinate along the wire. For small diameters the mechanical strength also becomes a problem and larger diameters are often used. The decrease concomitant the width of the operating plateau⁴ is as shown in fig. 4. Wires with 30 μm seem to be a good compromise and are the most frequently used.

In table 1 some properties of different materials are summarised.

Stainless steel wires are usually not antimagnetic due to method of production. This prevents their use in magnetic fields. They are also difficult to solder. Gold plated tungsten wires are most frequently used due to their strength properties. Since the wires are gold plated one has to be careful in soldering them. If the heat is too great the plating is destroyed. Therefore solder materials with low melting points ($\sim 140^\circ\text{C}$) should be used. In addition glueing the wire makes the connection even more reliable. To avoid heating entirely the wires are often crimped.

In order to prevent the effects of electrostatic and mechanical forces from bowing the wires beyond the desired tolerances the wires are stretched during installation. The amount of load depends on the chosen material and its diameter. For example for 30 μm W it is around 80 g.

Dealing with thousands of wires in the same gas volume it is necessary to check each wire after it is installed. Different methods are used. By measuring the resonance frequency the tension can be checked. Another possibility is to put a small weight on the wire and to measure the elongation.

For very long wires of several meters in chambers of small thickness an additional mechanical support is often used.

A necessary condition for good track measurements is exact positioning of the sense wire. For chambers at normal gas pressure the tolerances should be less than 100 μm . At larger pressures they should be as small as possible (10 to 30 μm). Different methods for positioning the wire will be shown in discussing different chamber types.

To avoid mechanical distortions with temperature variations it is desirable to use materials with almost the same expansion coefficient: Since aluminum is the usual material for support structures with an expansion coefficient of

23.8×10^{-6} per $^\circ\text{C}$ the choice of stainless steel and Cu-Be is favoured. If Cu-Be is tempered, it loses its undesirable tendency to curl up upon breaking. If W is used, the chamber should be assembled at the temperature expected during operation. In this respect the use of lucite in connection with aluminum is not the best choice. Different temperature coefficients may also cause serious trouble in making the chambers gas tight.

In the construction of large cylindrical chambers containing several thousands of wires under stress the support structure rigidity plays a large role. It will come to that in a moment.

In assembling the chamber components special care has to be taken. The hall or the room in which this is done should be practically dust free. Otherwise the dark current will be very high. In many cases it is desirable to clean the wires with alcohol after they are installed. Kinks, of course, should be avoided; they can cause mechanical breaks. If possible each wire should be individually tested electrically. In case of high dark current temporary inversion of the wire potential often helps.

After these general remarks about constructing chambers I would like to discuss specific chambers being successfully used in experiments. Since almost every set up in high energy physics uses drift chambers I can therefore select only a few examples.

Cylindrical drift chambers

Cylindrical chambers usually operate in axial magnetic fields in order to measure the momenta of charged particles over a large solid angle. The momentum is determined by the curvatures of the particles in the magnetic field. To detect the particles along their tracks many layers of cylindrical chambers of high accuracy are needed.

I would like to report on two versions operating successfully.

The first is a chamber⁵ constructed for a storage-ring experiment called TASSO at PETRA in Hamburg. It is in some respects similar to the central detector of MARK II at SPEAR. The dimensions of the set up are shown in fig. 5. 15 cylindrical chambers with radii from 36 to 128 cm are built around a beam pipe having a length of approximately 350 cm. The chamber consists of about 10000 wires under stress. The support structure is appropriately rigid. It consists of two 3.5 cm thick aluminum end plates separated by a 5 mm thick inner tube of fiberglass and epoxy and a 6 mm outer cylinder of aluminum. With all wires in-

stalled the distortion is less than 200 μm . The direction of the magnetic field is parallel to the cylinder axis.

The group decided to operate the chamber at atmospheric pressure. In order to obtain good spacial resolution the drift cell length should therefore be only a few cm, because at larger drift paths the effect of diffusion becomes important as I have shown in the previous section. On the other hand, since the costs of each wire are high the drift space should be as large as possible. Since the chamber has to operate in a magnetic field another factor has to be considered. The paths of the drifting electrons are effected by the magnetic field ($K_m \sim \vec{v} \times \vec{B}$). This results in a position and angle dependent time-space relation. At a known field this can be largely corrected with special electric field configurations. Also multiple measurements of the drift time along a single particle track can be used to partly correct these magnetic effects. Since the magnetic field is relatively small in this set up (0.5 T) the authors have used the cell configuration shown in fig. 6. Three wires sitting at the same potential on each side of the sense wire are used for shaping the electric field. The black lines indicate the paths of the drifting electrons under the influence of the electric and magnetic field.

Fig. 7 shows the arrangement of the different cell layers. To measure the coordinate parallel to the cylinder axis the wires of two neighbouring layers are tilted by a small angle. The measured resolution of this configuration is $\sigma_x = 200 \mu\text{m}$ and $\sigma_z = 2 \text{ mm}$.

What special tricks were used in constructing these chambers? Fig. 8 shows how the positioning of the wire is accomplished. The sense wire is fed through a brass tube held in an insulator. The ends of the wire are soldered and glued to a pin. The alignment of the wire is provided by a small piece which is made with 50 μm tolerance. The insulator is of high quality (Hostaform C).

The mounting of all cell components is done at constant temperature to avoid the problems of differential thermal expansion. Extreme care was taken concerning cleanliness. The technical staff wore clothes like doctors in an operating room as shown in fig. 9, which illustrates the mounting of the wires. Each wire was mechanically and electrically inspected as I have already discussed. When two, sometimes three, drift-chamber layers were completed they were covered by a 5 mm selfsupporting layer of foamed lucite called Rohacell 31 with thin aluminum foils (20 μm) on each side. This protects them from being destroyed or being contaminated by dust. As the density is only $\rho = 0.03 \text{ g cm}^{-3}$ this extra

material does not effect the momentum resolution very much but alters the electric field configuration slightly.

A drift chamber set up requiring even more accurate construction is the JET chamber built by the Heidelberg group of Heintze at al.⁶ for use in the JADE experiment at PETRA.

The JET chamber is also a cylindrical chamber which operates within an magnetic field of 0.5 T, but in contrast to TASSO is a high pressure chamber. It is specially designed to distinguish and measure large numbers of closely spaced tracks. The Heidelberg group therefore decided to use a gas mixture at 4 atm. With this increased pressure the width of the sense wire pulse decreases. Therefore particles as close as 7 mm apart can be distinguished. High pressure also reduces the influence of diffusion as we have seen in the discussion of the physical limits. This permits use of a large drift path without losing too much in positioning accuracy. In addition a measurement of dE/dx is made to determine the specific ionisation and hence the mass of the particle. Sufficient dE/dx resolution requires that the charged primary particle produces a large number of ions in passing through the sensitive chamber volume, a requirement also helped by the high pressure.

The JET chamber consists of a pressure vessel containing 86 cells concentrated in three rings around the beam pipe (fig. 10). The length of the detector is 240 cm. To handle this configuration more easily the total surface is divided into 24 segments each containing 4 cells. Each cell has 16 sense wires (fig. 11). To obtain a constant electric drift field, specially arranged field electrodes on Kapton foils are placed at the cell walls. This configuration allows measurement of x, y, z position and the energy loss ΔE of the primary particle. x is measured by the drift time. y is determined by the position of the sense wire. The z-coordinate is obtained by charge division method. To obtain a large value of the wire resistance they used a diameter of the sense wire of 20 μm . To determine the number of electrons produced by the primary charged particle the signals on both ends are added to correct for the attenuation.

The left-right ambiguities are resolved by staggering the wires as shown in fig. 12. Two succeeding sense wires are displaced alternately by a distance δ in opposite directions with respect to the cathode wires. The ambiguity is resolved by computing $(\Delta z_{\text{even}} - \Delta z_{\text{odd}}) / v = \pm 2 \delta$. From the sign one can distinguish the sides. δ should be as small as possible since it can cause displacement of the wires due to the electric field. It has been chosen to be 150 μm .

Fig. 13 shows the resulting resolution of the left-right ambiguity. The tracks on both sides are clearly separated. The spacial resolution is $150 \mu\text{m}$ including the effects of a $40 \mu\text{m}$ wire displacement due to electrical forces.

What are the special problems in the performance of a chamber at high pressure? Fig. 14 shows schematically the mechanical structure of a segment. The endplates, which are made of aluminum, suffer a deformation of less than $25 \mu\text{m}$ under the force of the wires. To fix the length and make the whole configuration stable, four support beams are used. To reduce the material seen by the jet particles these beams consist of a sandwich of $100 \mu\text{m}$ aluminum foils and Rohacell plexiglass foam. The straightness of this configuration is kept better than $300 \mu\text{m}$. In order to maintain the excellent resolution and resolve the left-right ambiguity at all positions inside the chambers, all wires must sag uniformly due to gravitational forces. Using different materials and diameters the wires have to be stretched differently ($60, 600 \text{ g}$, respectively). The sagging is $70 \mu\text{m}$ and the deviation for different wires is less than $7 \mu\text{m}$. The positions of the wires are determined by notches in a machinable ceramic called Macor. The relative accuracy of these positions in one cell is about $10 \mu\text{m}$. The wires are soldered to a printed board mounted on the ceramic. Four brass dowels on each side of a segment guarantee that adjacent segments are aligned better than $20 \mu\text{m}$.

The chamber was mounted under similar conditions as discussed in the TASSO set up. The JET chamber has now operated about one year and has proved its reliability. It is a good tool for looking for new physical phenomena at the PETRA-storage ring.

Planar drift chambers

The next category of chambers I would like to discuss is the planar chamber, which is also often used in connection with magnetic fields to measure the momenta of particles. They are usually placed not in, but before and behind analyzing magnets. To assure a good momentum resolution these chambers should measure the particle track very accurately in planes separated by as much distance as possible. In order to reduce multiple scattering these chambers should also contain as little material as possible. Therefore chambers at large pressure placed inside thick wall pressure vessels cannot be used. Chambers at atmosphere pressure allow thin foils to seal the gas volume.

One example of this chamber type consists of two half circles sitting around a beam pipe. It will be built into the PLUTO forward spectrometer for measurements of $\gamma\gamma$ -reactions at PETRA.

To get optimum spacial resolution and to tolerate the expected counting rates the drift path is chosen to be 1 cm . The thickness of a cell is also 1 cm . The left-right ambiguities are resolved by a second layer shifted by half a cell width. A second double layer rotated by 90° measures the second coordinate. A third double layer operating in the proportional chamber mode resolves the possible ambiguities caused by multiple particle hits.

The required mechanical accuracies of about $50 \mu\text{m}$ are determined by a special shaped 15 mm thick support frame (fig. 15). On this frame there are 4 alignment pins serving as reference points for all wire layers. The wires of each layer are soldered to an especially rigid type of printed board called Stesalite. The frame is cut out of a 5 mm solid plate which also serves as spacer between adjacent wire layers. To avoid disturbing the solder joints of the wires the printed board provides a separate pad for soldering the connection to the preamplifiers.

In high accuracy chambers it always is interesting to see which method is used to position the sense wires exactly. In this case the alignment is done by hand using the aid of a microscope on a measuring table. The cathode wires are fixed on a similar etched frame. Since these wires do not need to be as accurately positioned as the former ones they are aligned using the transfer frame technique. The spacial resolution is better than $200 \mu\text{m}$ on the average. Including the mylar foils (0.1 mm) which seal the gas volume a crossing particle sees only $4 \cdot 10^{-3}$ radiation lengths of material.

In high energy physics large area detectors covering several hundred m^2 and having reasonable space resolution are often needed. One example is a μ detector consisting of chambers placed behind a thick wall of absorbing material.

The counting rates are usually not high. The expenses for such a device can be kept low by using drift chambers with large drift cells.

Since the costs for time measuring devices are not small the amplifier output of several wires can be orred and fed into the same TDC input. An inexpensive flipflop connected to each sense wire indicates from which wire the time measurement stems.

I would like to report on such a system developed for the PLUTO detector. One of the main principles in producing these chambers was to use mass production techniques as much as possible since man power is getting more and more expensive. This also increases the reliability of the whole system.

Each chamber consists of four drift cells arranged in two layers. The layers are displaced with respect to each other by half the cell width to resolve the left-right ambiguities. The units are small enough to fit into almost all geometrical configurations. Smaller units would cost more for high voltage distribution and electronics. The body of the four cells is a specially designed extruded aluminum profile and is shown in fig. 16. The U and I beams on both sides of a plate guarantee a rigid structure. These profiles fix almost all dimensions. The maximum drift length is 8 cm which is determined by the repetition rate of PETRA. To be fully efficient along the whole cell the drift field must be shaped with an arrangement of conducting strips. The minimum number of strips is given by the tolerable difference of $E_{\max} - E_{\min}$ determined by the plateau of the saturated drift velocity. Fig. 17 shows that no more than 5 strips are needed.

Such conducting strips are often produced from printed board material (etched G10 for example). G10 is not effected by any of the known gas mixtures but it is rather expensive. To reduce the costs polystyrol sheets were employed as a support for inexpensive selfadhesive 25 μ m aluminum field shaping strips. Polystyrol is a very cheap material commonly used for food containers, such as Joghurt. Extensive tests have shown that this material will not poison the chamber gas. The field shaping elements were fabricated using mass production techniques. In glueing the field shaping elements into a cell only minimum care is needed. A 1 mm thick aluminum sheet which also holds field chaping elements is glued to the top of each double chamber.

The end pieces with the wire positioning elements and the strip voltage supply is shown in fig. 18. To avoid soldering, the connections to the strips are made by Cu-Be springs. This enables the use of inexpensive insulating materials such as Delrin which is also easier to machine. In the lower chamber the sense wire positioning is shown. The wire is soldered into a brass tube with a 0.5 mm inner diameter.

To show that such a simple configuration works satisfactorily the measured time-space relations for particles with incident angles of 0° and 55° with respect to the normal of the chamber plane are shown in fig. 19. As is shown in fig. 20, the chamber has an almost 100 % efficiency over the whole drift path. Fig. 21 demonstrates the reasonable space resolution of the detector.

Acknowledgement

I gratefully acknowledge the support and hospitality of the DESY directorate and would like to thank Prof. J. Heintze, Dr. U. Kötze and Dr. G.G. Winter for their invaluable cooperation in discussing their experimental set up. I am indebted to Dr. R. Kellogg for many discussions and reading the manuscript. Finally I wish to thank Mrs. R. Siemer and Mr. P. Burmeister for excellent technical support.

Table 1

	W (Re)	Mo	stainless steel	Cu-Be2
γ kp mm ⁻²	$41 \cdot 10^3$	$30 \cdot 10^3$	$20 \cdot 10^3$	$13 \cdot 10^3$
$\frac{\Delta L}{L} \cdot \frac{1}{\Delta T}$ 10^{-6} C^{-1}	4.4	5.3	16	17
tensile strength kp mm ⁻²	180 - 410	140 - 250	60	30 - 130
remarks	most used wires		not antimagnetic	

References

- 1) W. Sauli, CERN 77-09
- 2) G. Schulz et al., Nucl. Instr. and Meth. 151 (1978) 413
- 3) W. Farr et al., Nucl. Instr. and Meth. 154 (1978) 175
- 4) G. Morel et al., Nucl. Instr. and Meth. 141 (1977) 43
- 5) B. Boerner et al., this conference
- 6) W. Farr et al., Nucl. Instr. and Meth. 156 (1978) 283
J. Heintze, Nucl. Instr. and Meth. 156 (1978) 227
H. Drumm et al., this conference

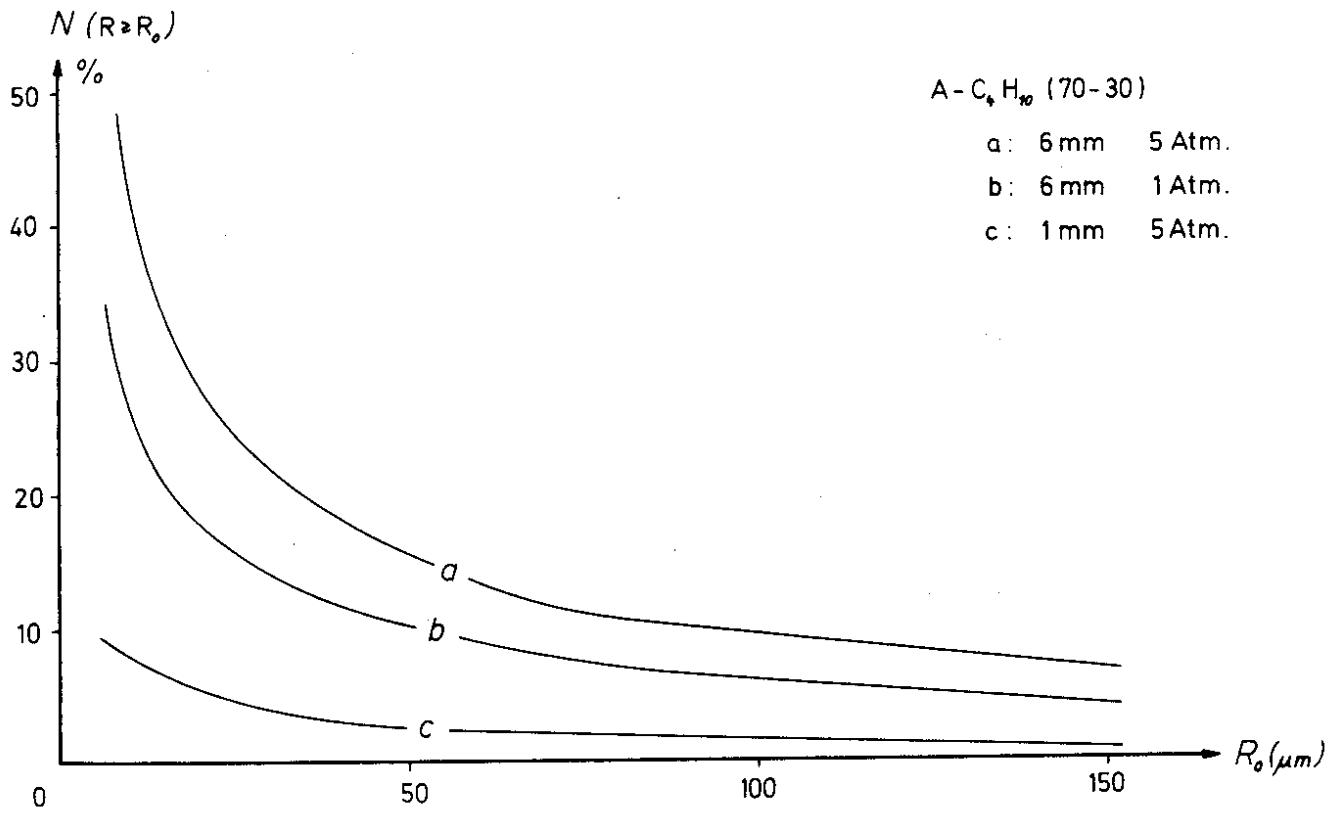


Fig. 1

Figure Captions

- Fig. 1 Number of electrons with a range larger than R_0 produced by minimum ionising particles.
- Fig. 2 Space resolution as a function of the drift length x .
- Fig. 3 Space resolution for different gas pressures.
- Fig. 4 Operating plateau.
- Fig. 5 Cylindrical drift chamber of the TASSO detector.
- Fig. 6 Cell configuration of the TASSO chamber in a magnetic field.
- Fig. 7 Arrangement of the drift cells of the TASSO chamber.
- Fig. 8 Positioning of sense wire of the TASSO chamber.
- Fig. 9 Mounting of wires in the TASSO chamber.
- Fig. 10 Front view of detector elements of the JET chamber (JADE).
- Fig. 11 Drift cell of the JET chamber.
- Fig. 12 Wire staggering in the JET chamber.
- Fig. 13 Resolution of right-left ambiguity in the JET chamber.
- Fig. 14 Mechanical structure of a segment of the JET chamber.
- Fig. 15 Planar chamber of the PLUTO detector.
- Fig. 16 Cell configuration of the PLUTO μ detector.
- Fig. 17 The maximum and minimum electric field for different strip numbers.
- Fig. 18 Side view of the μ detector.
- Fig. 19 Time-space relation for minimum particle of 0° and 55° incident angles.
- Fig. 20 Efficiency as a function of the drift path.
- Fig. 21 Space resolution for different drift paths.

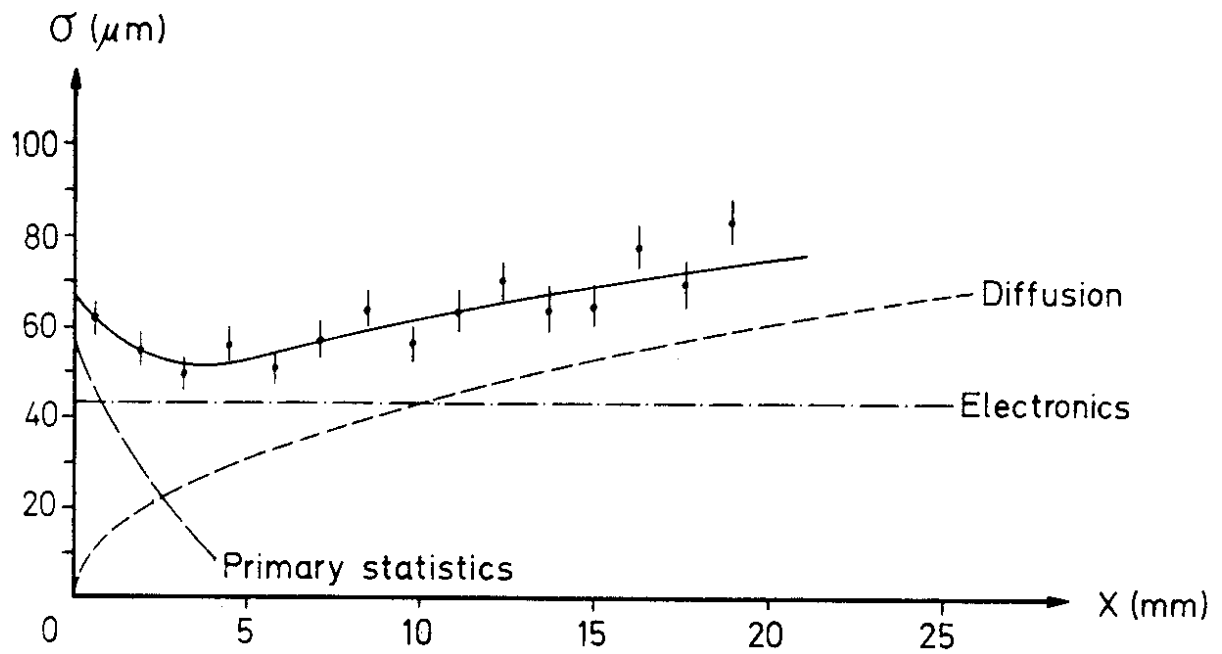


Fig. 2

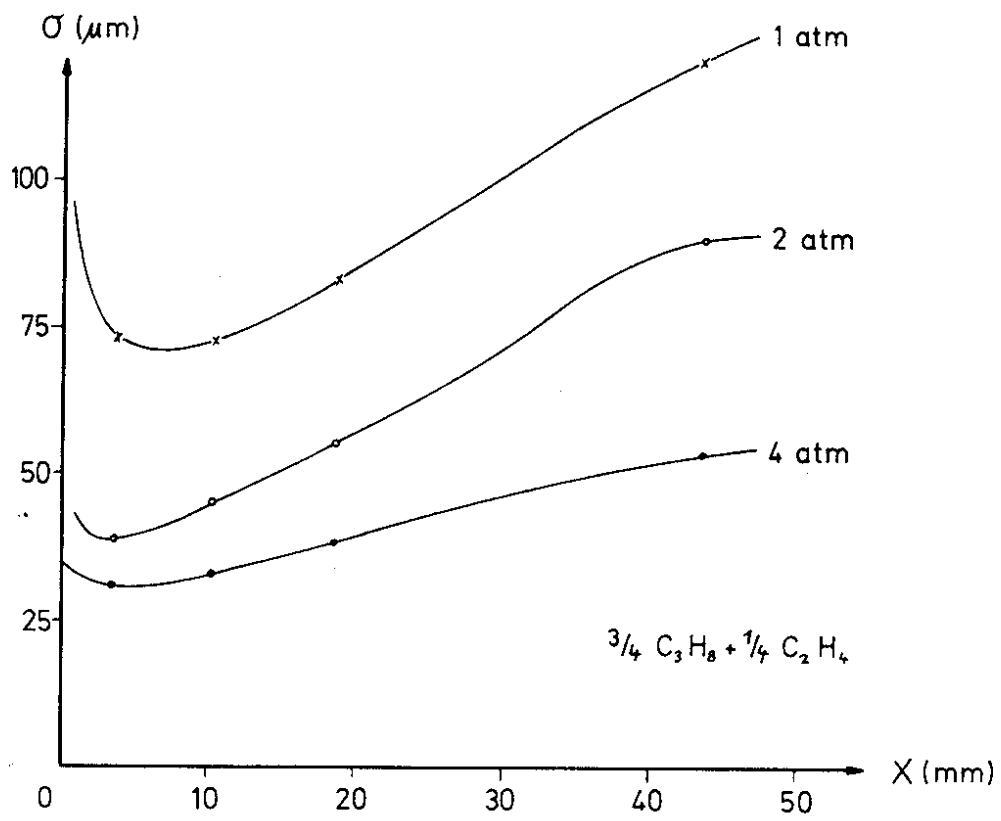


Fig. 3

Gas mixture Argon 70 % Isobutane 30 %

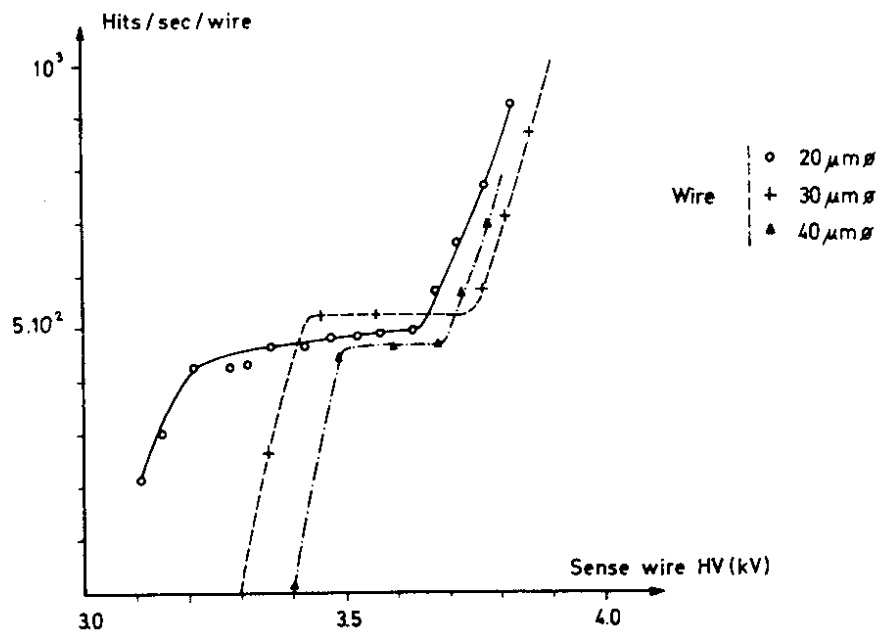
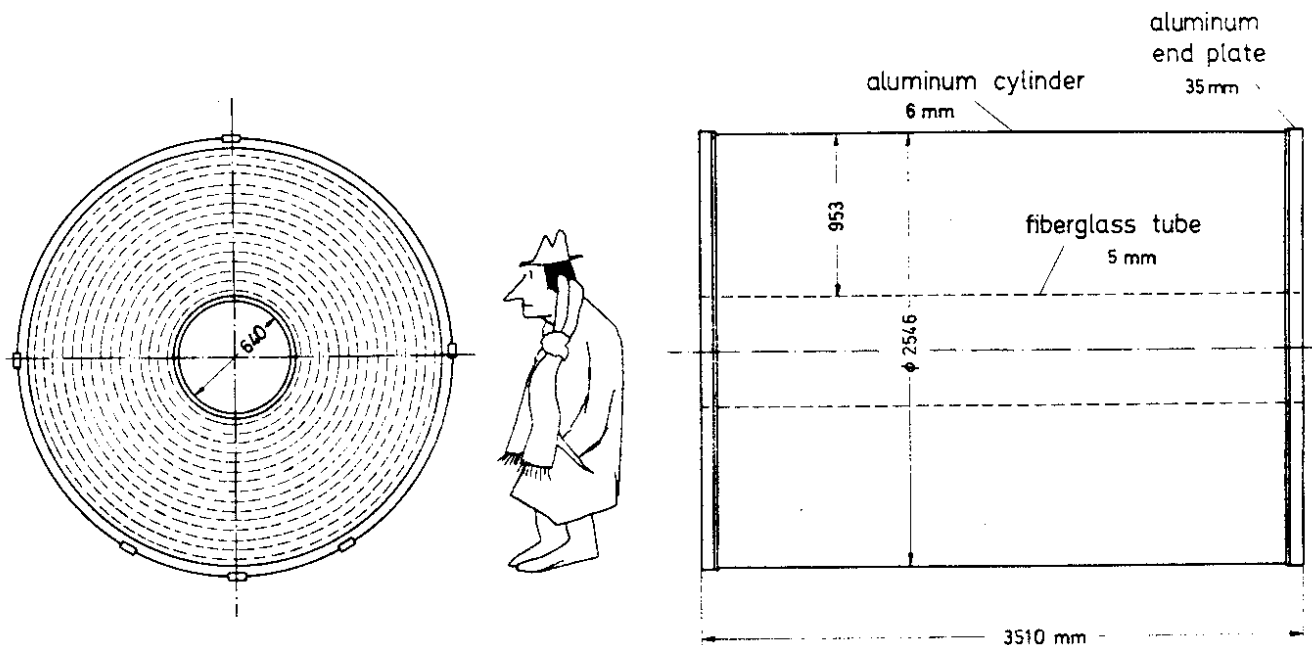


Fig. 4



TASSO

Fig. 5

TASSO

drift cell

$B = 0,5$ Tesla

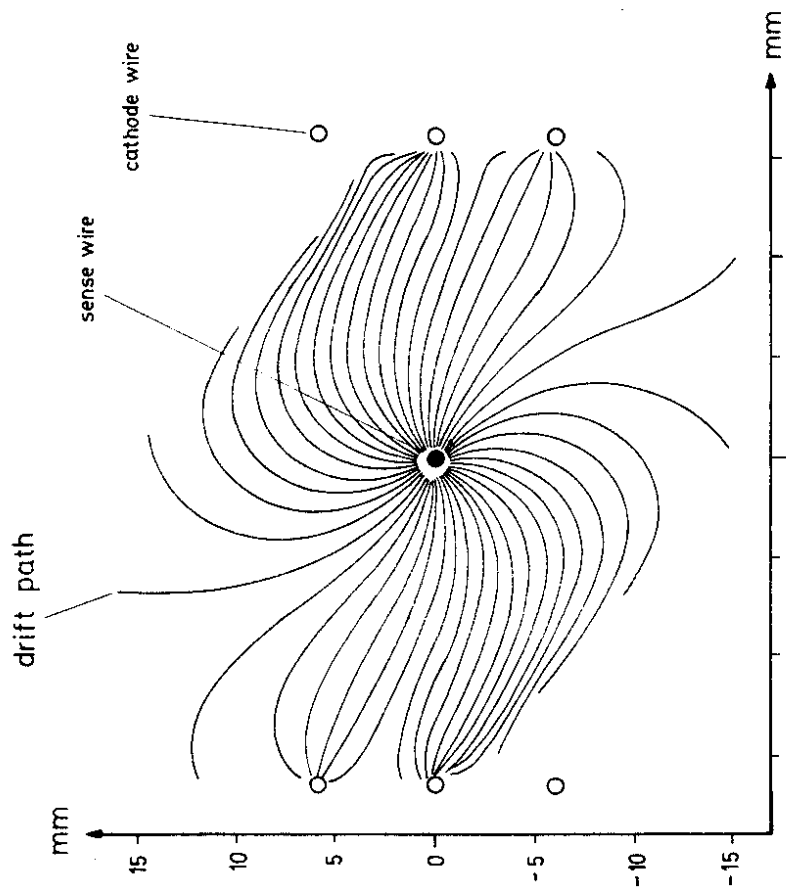


Fig. 6

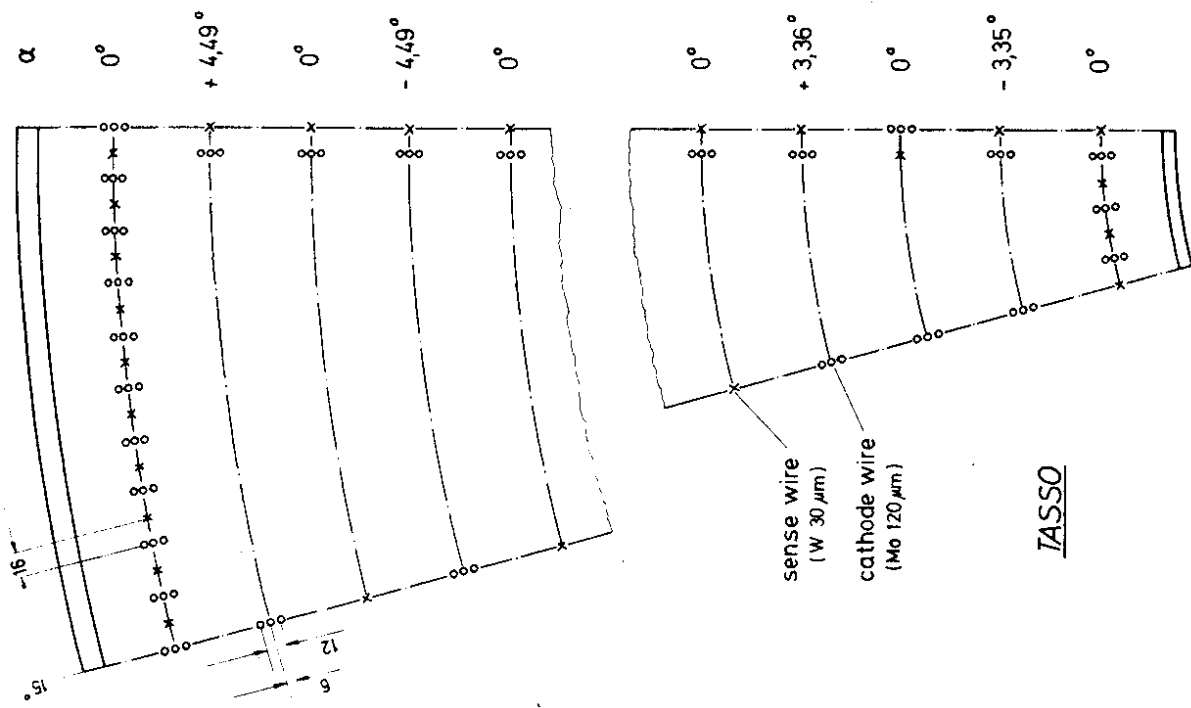


Fig. 7

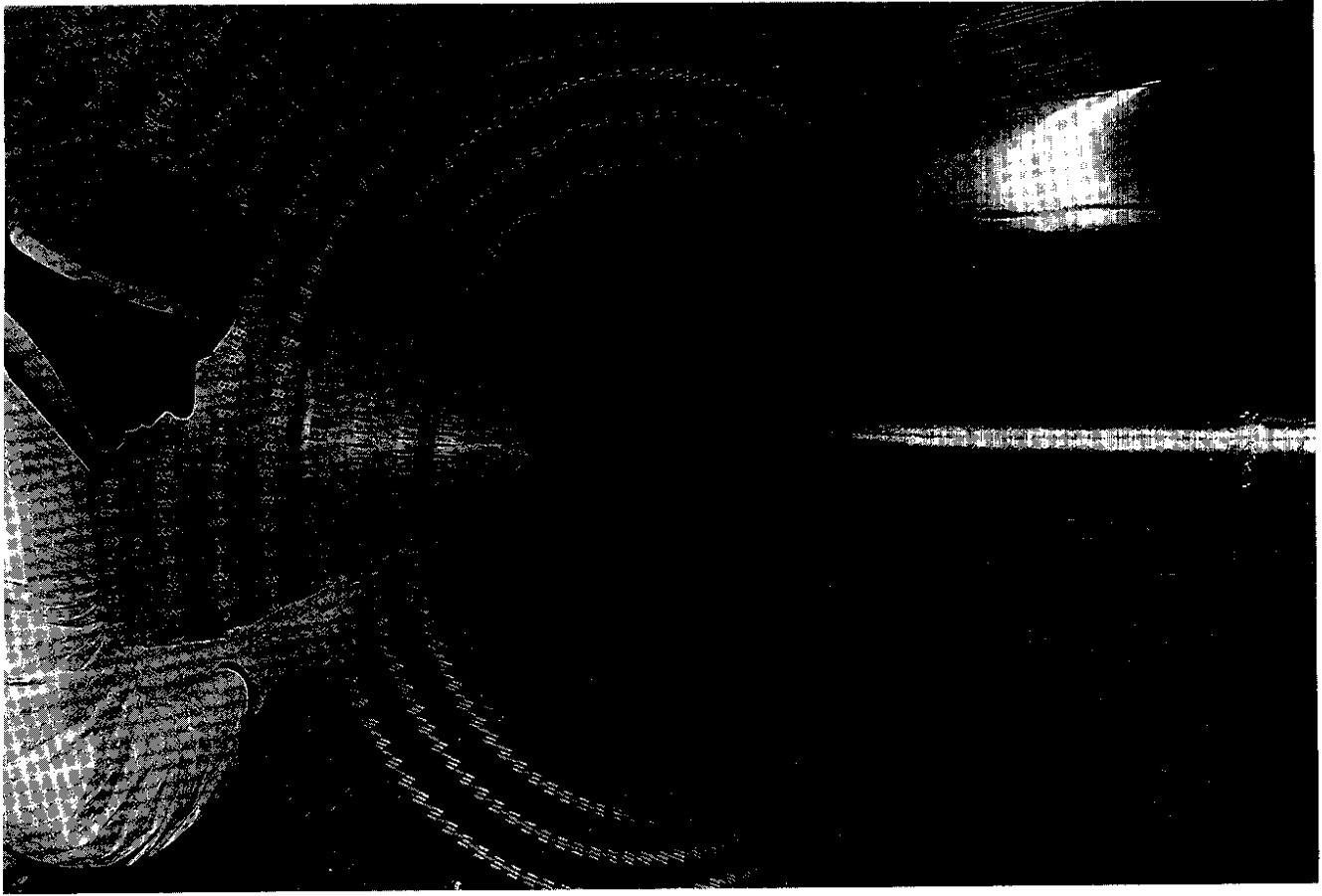


Fig. 9

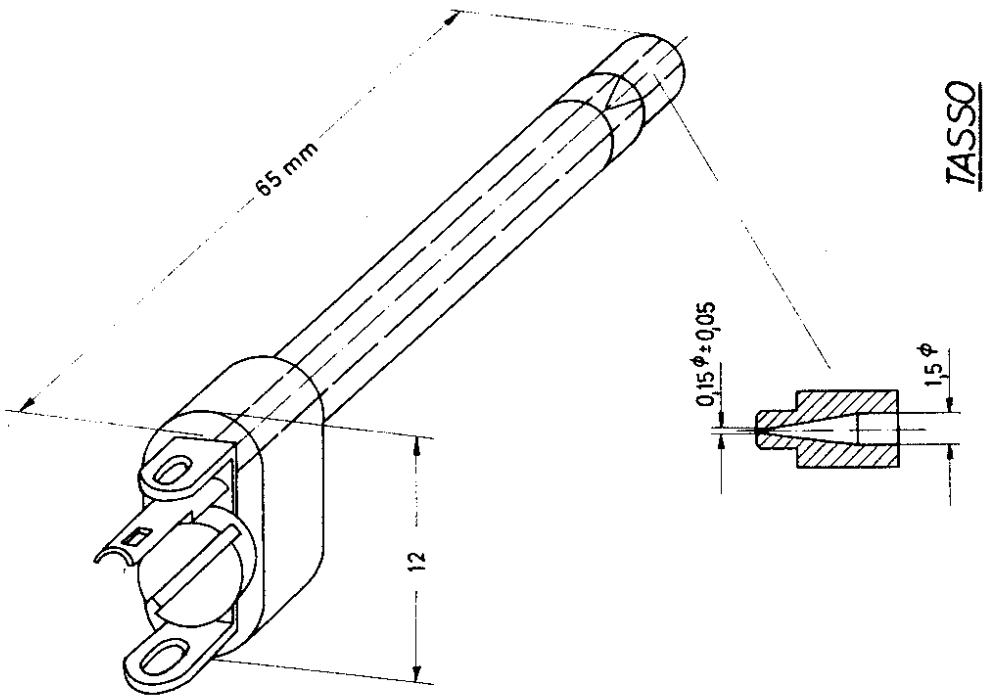


Fig. 8

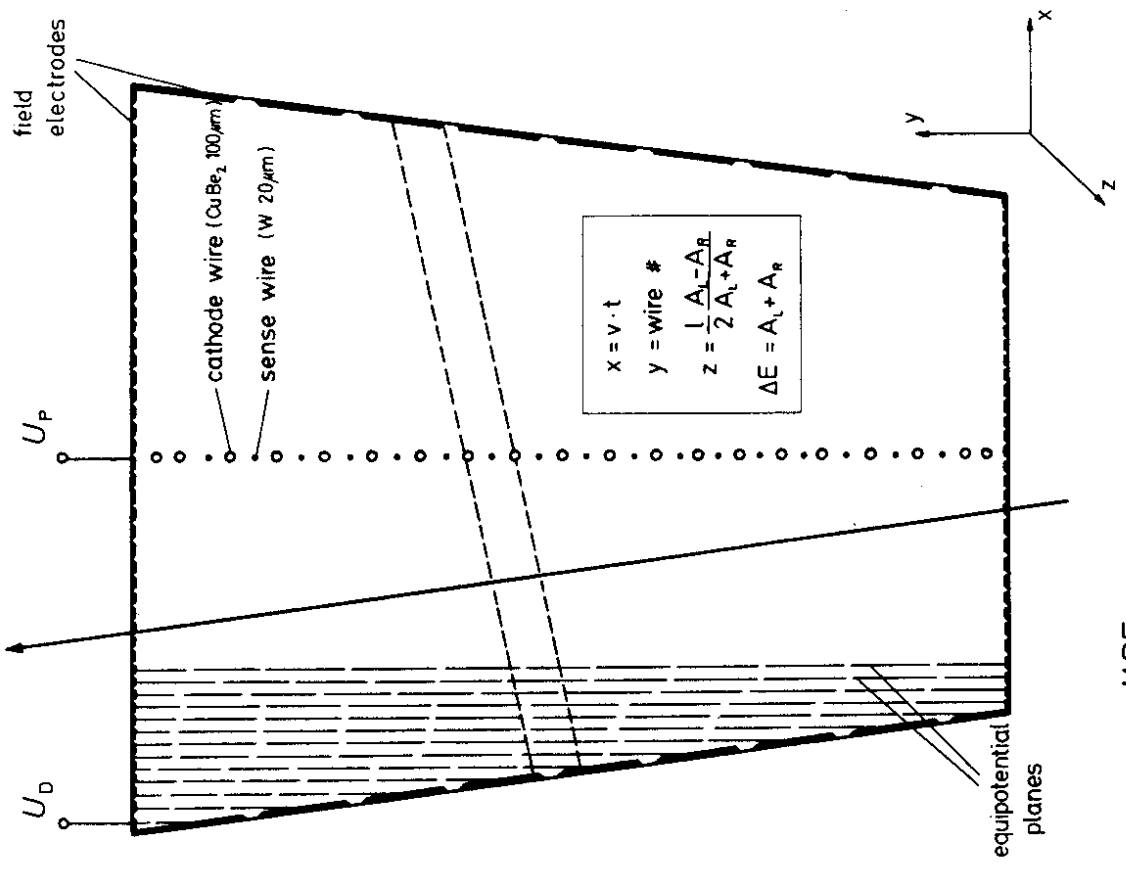
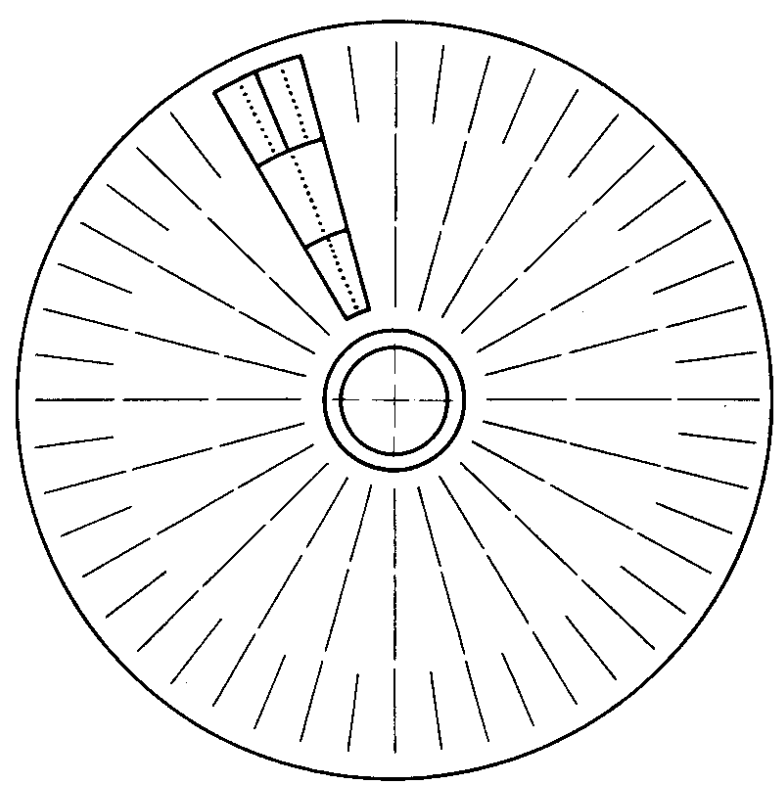


Fig.11

JADE



24 segments (each 4 cells)
 16 sense wires/cell → 1536 wires
 $R_1 = 21$ cm
 $R_{wp} = 79$ cm
 $L = 240$ cm

Pressure : 4 Atm.

Ar	CH ₄	i-butane
90 %	8.5 %	1.5 %

Fig.10

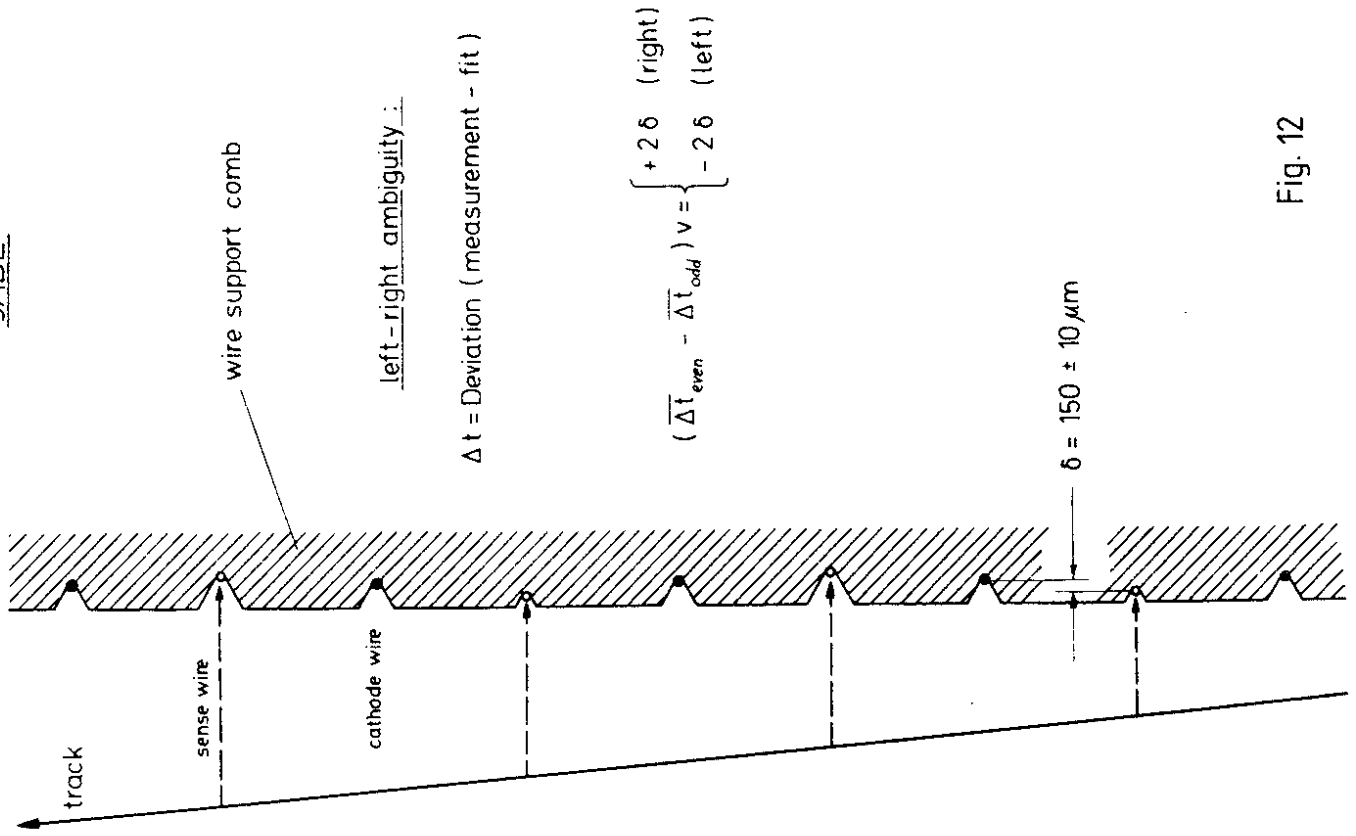
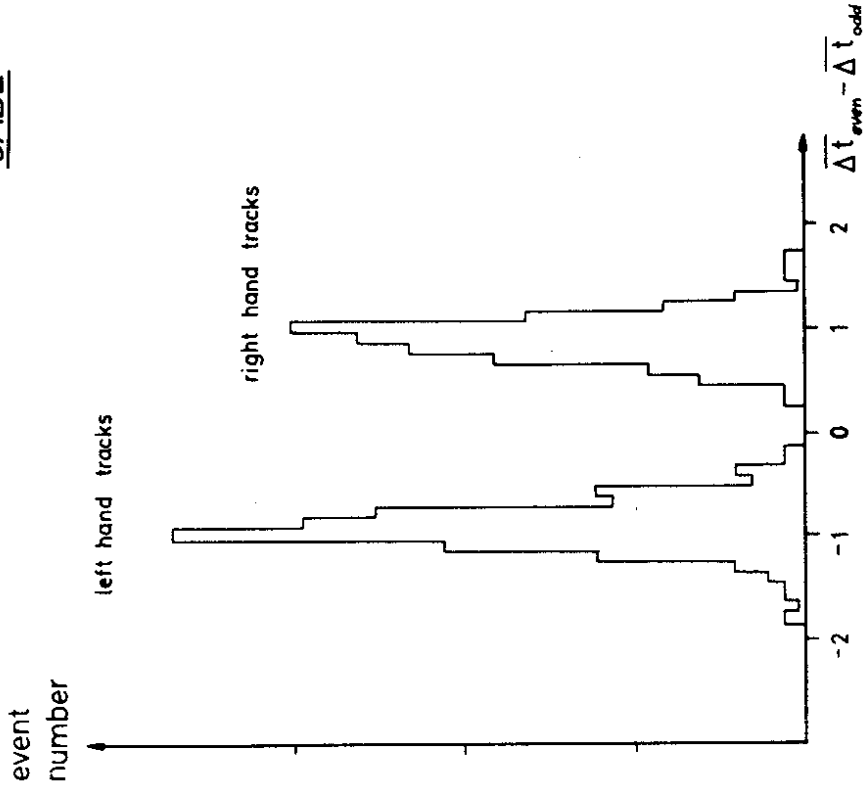


Fig. 12



1 unit $\hat{=}$ 380 $\mu\text{m} \approx 2.6$

150 μm mech. + 40 μm el. stat.

Fig. 13

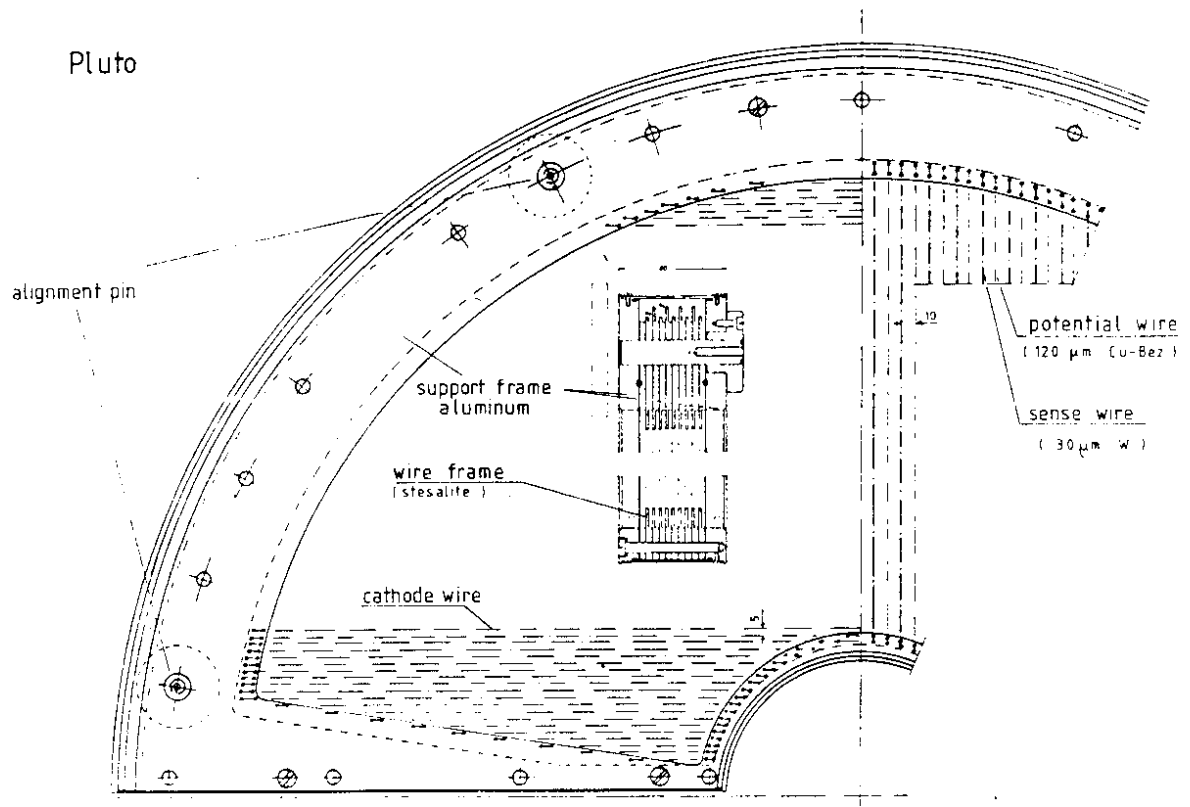


Fig. 15

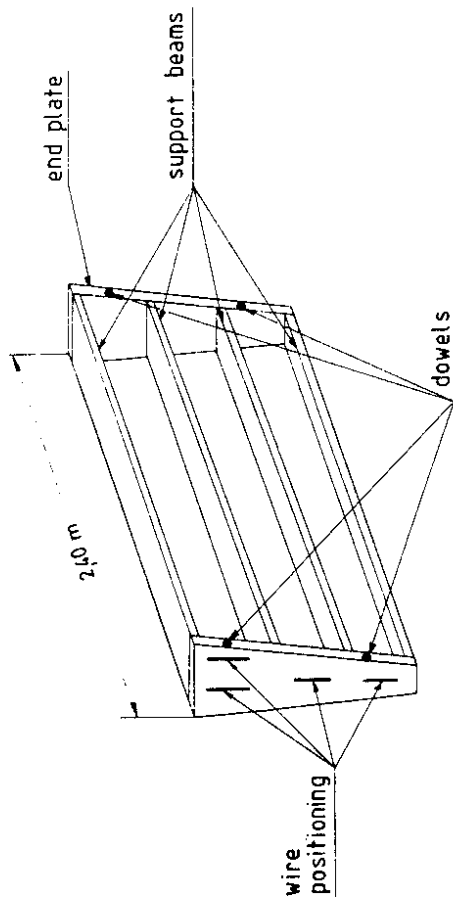


Fig. 14

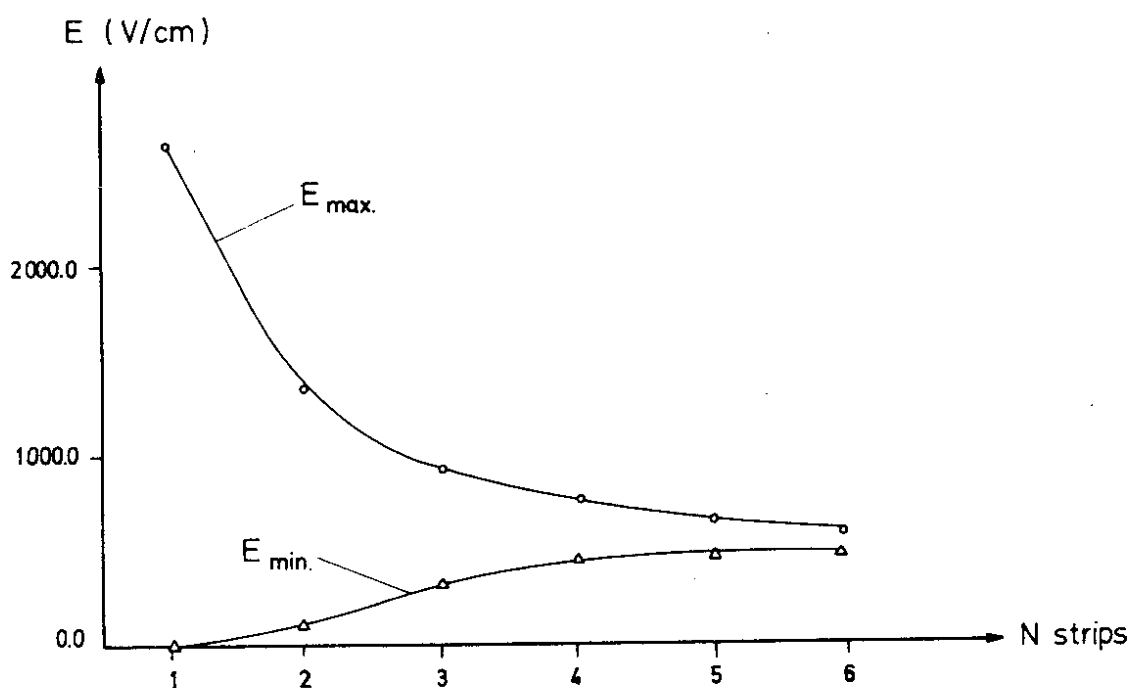
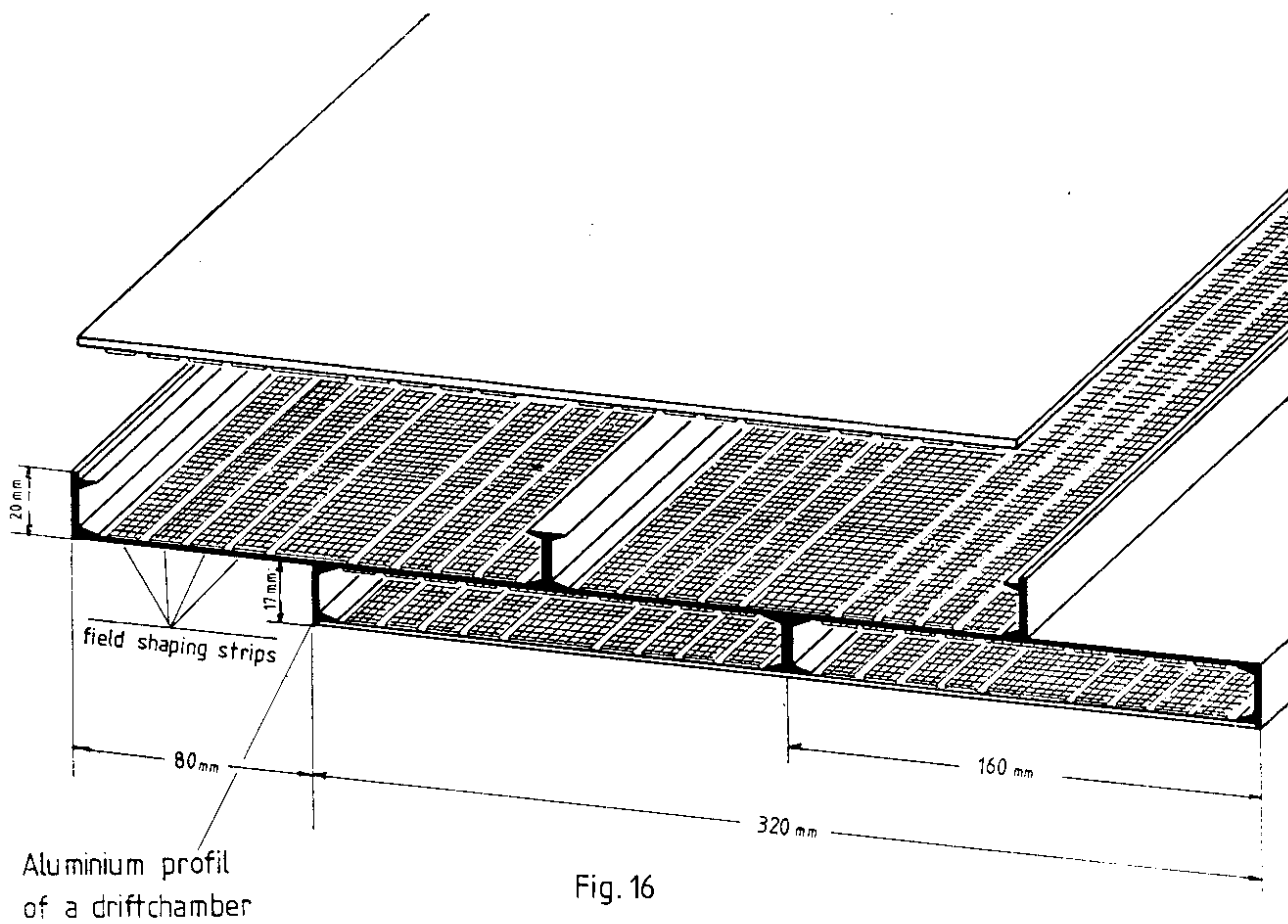


Fig. 17

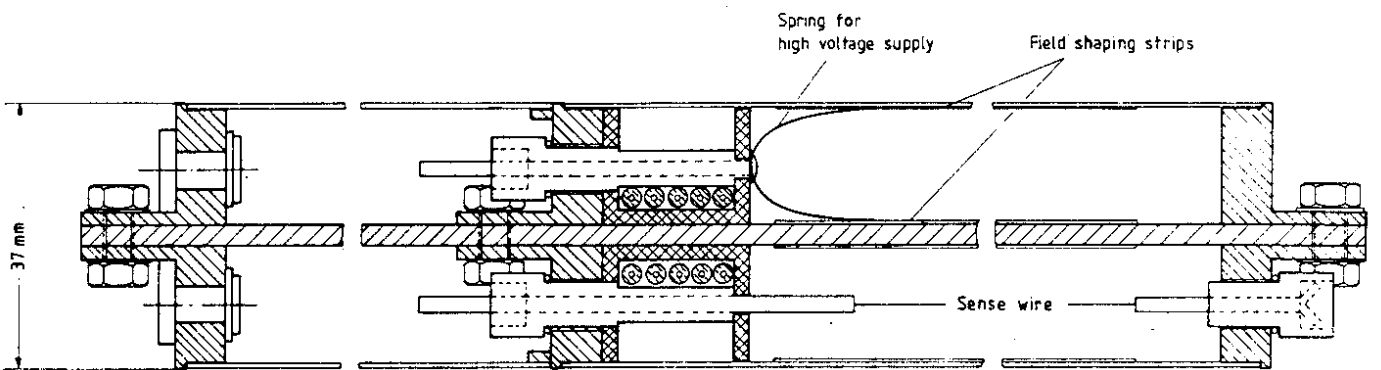


Fig. 18

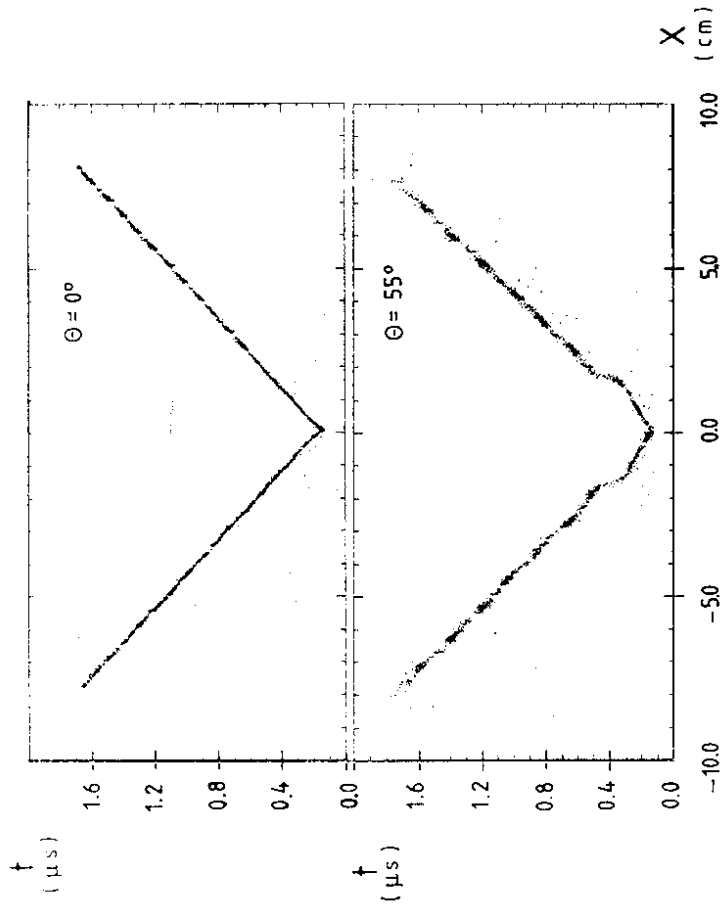


Fig. 19

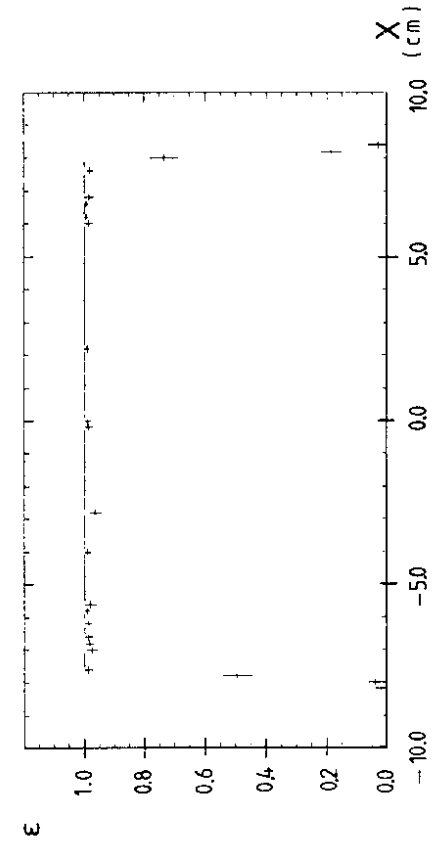


Fig. 20

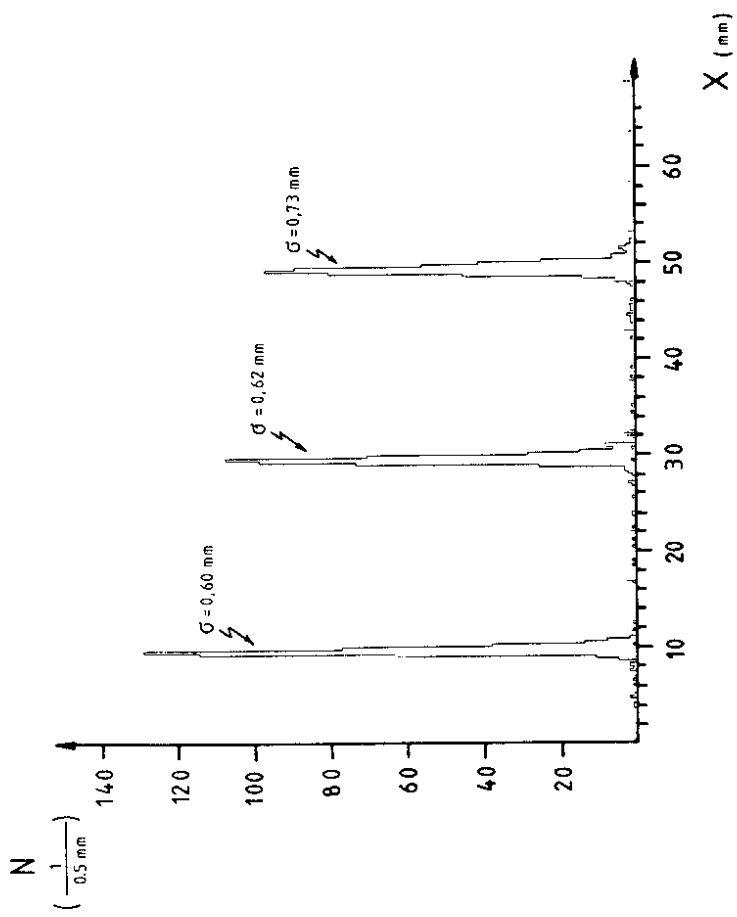


Fig. 21

